Asymptotic time dependence in the fractal pharmacokinetics of a two-compartment model

P. Chelminiak,* R. E. Marsh, and J. A. Tuszyński
Department of Physics, University of Alberta, Edmonton, Alberta, Canada, T6G 2J1

J. M. Dixon
Department of Physics, University of Warwick, Coventry, CV4 7AL, United Kingdom

K. J. E. Vos
Department of Physics, University of Lethbridge, 4401 University Drive, Lethbridge, Alberta, Canada, T1K 3M4
(Received 4 August 2004; revised manuscript received 6 January 2005; published 9 September 2005)

We further investigate, both analytically and numerically, the properties of the fractal two-compartment model introduced by Fuite *et al.* [J. Fuite, R. Marsh, and J. Tuszynski, Phys. Rev. E **66**, 021904 (2002)]. Specifically, we look at the effects of the fractal exponent of the elimination rate coefficient on the long-time behavior of the pharmacokinetic clearance tail. For small exponent values, the tail exhibits exponential behavior, while for larger values, there is a transition to a power law. The theory is applied to seven data sets simulating drugs taken from the pharmacological literature.

DOI: 10.1103/PhysRevE.72.031903 PACS number(s): 82.39.−k, 05.45.Df, 61.43.Hv, 82.30.−b

I. INTRODUCTION

Pharmacokinetics is the study of the absorption, distribution, metabolism, and eventual elimination of a drug from the body [1]. Pharmacological data, which usually consist of the concentration of a drug in the plasma or blood as a function of time, are commonly described using compartmental models [2]. In these models, the body is divided into a collection of compartments, and a drug's journey between two different compartments is described by a rate coefficient. Figure 1 shows an example of a two-compartment model, where C_1 denotes the concentration in the first compartment (representing, for example, the circulatory system) and C_2 denotes the concentration in a peripheral compartment (such as the liver). The drug is introduced into the first compartment at a rate f, is reversibly transferred between the two compartments, and is finally excreted from the system through the second compartment. The coefficient k_{ij} represents the fractional transfer rate from compartment i to compartment j. In the case when all the coefficients are constant (representing well-stirred conditions), we obtain the following set of differential equations:

$$\dot{C}_1 = k_{21}C_2 - k_{12}C_1 + \frac{f}{V_d}, \tag{1}$$

$$\dot{C}_2 = k_{12}C_1 - (k_{21} + k_{20})C_2, \tag{2}$$

where f is the infusion rate of the drug into the system and V_d is the theoretical volume of distribution into which the dose is dispersed. To obtain an equation in C_1 alone, we first differentiate Eq. (1) with respect to time to give

$$\ddot{C}_1 = k_{21}\dot{C}_2 - k_{12}\dot{C}_1, \tag{3}$$

where f/V_d has been assumed to be constant in time. Equation (2) is now used to eliminate $\dot{C}_2$ to give

$$\ddot{C}_1 = k_{21}(k_{12}C_1 - (k_{21} + k_{20})C_2) - k_{12}\dot{C}_1. \tag{4}$$

The term in C_2 in Eq. (4) may now be replaced in terms of C_1, C_1, and f using Eq. (1) so that

$$\ddot{C}_1 = k_{21}k_{12}C_1 - k_{21}(k_{21} + k_{20})\left\{\dot{C}_1 + k_{12}C_1 - \frac{f}{V_d}\right\}\frac{1}{k_{21}} - k_{12}\dot{C}_1. \tag{5}$$

Rearranging the terms in Eq. (5) gives the second-order equation

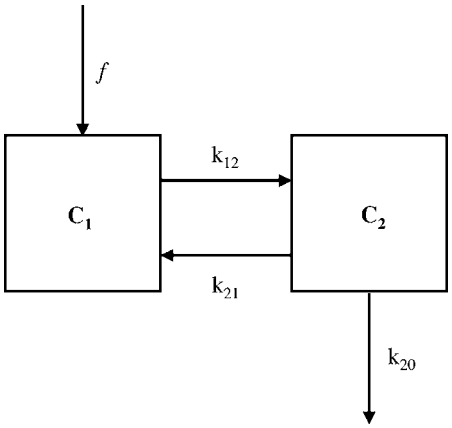

FIG. 1. Schematic representation of a two-compartment model with input at a rate f into compartment 1, reversible transfer between the two compartments, and elimination from compartment 2.

*Permanent address: Faculty of Physics, A. Mickiewicz University, Umultowska 85, 61-614, Poznan, Poland.

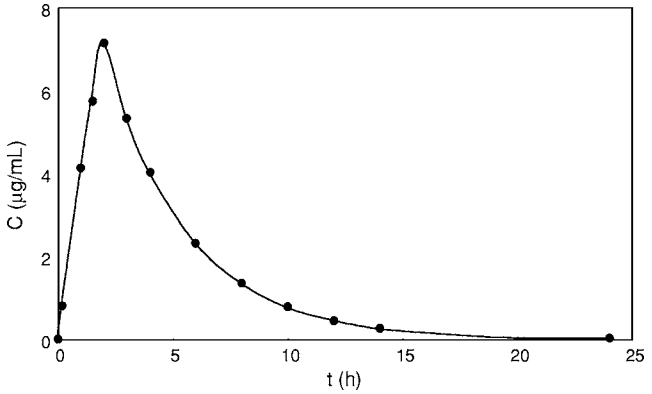

FIG. 2. A pharmacokinetic profile of drug concentration C as a function of time t, generated using Eq. (1) with the following values chosen for illustration: $k_{12}=0.5\ h^{-1}$, $k_{21}=1.0\ h^{-1}$, $k_{20}=1.5\ h^{-1}$, and $V_d=10.0\ L$.

$$\ddot{C}_1 + (k_{12} + k_{20} + k_{21})\dot{C}_1 + k_{12}k_{20}C_1 = \frac{f}{V_d}(k_{21} + k_{20}). \quad (6)$$

For bolus infusions, f can be replaced by

$$f(t) = \begin{cases} D & t = 0, \\ 0 & t > 0. \end{cases} \quad (7)$$

The homogeneous component of the solution of Eqs. (6) and (7) can be taken as a sum of terms that are exponential in time.

Figure 2 shows a typical graph of the concentration in the first compartment as a function of time. There is an initial rise as absorption of the drug dominates. After reaching a maximum concentration, the curve decreases in a long tail as elimination of the drug dominates. The shape of this elimination tail is important in determining the clearance of the drug from the system.

The classical compartmental model is based on two main assumptions: each compartment must be homogenous (there is instantaneous mixing), and the rate coefficients are all constant (the fraction of drug transferred between any two compartments does not vary with time). However, these assumptions frequently fail under physiological conditions, which, by their nature, impose geometric constraints. For example, the circulatory system consists of a series of bifurcating vessels, and the time it takes for a circulating drug to reach its target will depend on its path. Similarly, most organs in the body are complex structures that can be characterized by hierarchically organized networks, and the diffusion of a drug through them will be limited by the geometry of the available surfaces.

It has been shown that physical systems under geometric constraints exhibit both anomalous diffusion and anomalous reaction rates. For a particle diffusing through a heterogeneous medium, its average mean-square displacement $\langle r^2(t)\rangle$ as a function of time is given by the power law [3]

$$\langle r^2(t)\rangle \sim t^{2/(d+2)},$$

where d is the fractal dimension. Anacker *et al.* [4] and Anacker and Kopelman [5] reported results of their computer simulations for fractal chemical kinetics, leading to the introduction of time-dependent kinetic rate coefficients. For heterogeneous chemical reactions (for example, ones that occur on or inside a fractal medium), the rate coefficient has been found to be a decreasing power of time [6,7],

$$k(t) = k_0 t^{-\alpha}, \quad (8)$$

where α is the heterogeneity, or fractal, exponent and can be expressed in terms of the spectral dimension d_s as follows:

$$\alpha = 1 - \frac{d_s}{2}. \quad (9)$$

In pharmacokinetics, homogeneous conditions are considered "well stirred" and heterogeneous conditions near tissues are considered "understirred" [8]. While the homogeneous portions of the circulatory system can be described using conventional kinetics, regional volumes such as those feeding the liver are fractal and thus should be governed by fractal kinetics.

Weiss [9] incorporated long-time fractal trapping kinetics into a noncompartmental circulatory pharmacokinetic model, an approach that is perhaps best suited for low-clearance drugs. Other approaches include the homogenous-heterogeneous distribution model introduced by Macheras [10] to take into account the global and regional natures of blood flow to organs. Karalis *et al.* [11] and Karalis and Macheras [12] developed the concept of a fractal volume of distribution and applied it to a number of drugs. They found that in most cases, there was a significant difference between the fractal volume and the conventional volume of distribution. Furthermore, they found that the fractal volume of distribution scales almost linearly with body mass.

Fractal rate coefficients can be incorporated into a compartmental model through the use of Eq. (8). The model remains linear, but the fractal rate coefficients introduce a time dependence. In the first quantitative application of a fractal compartmental model, Fuite *et al.* [13] incorporated the physical structure of the liver, the organ responsible for eliminating the cardiac drug mibefradil [14]. The hepatic microvascular system consists of a series of bifurcating vessels that follow particular scaling laws, with an estimated spatial fractal dimension of around 2 [15]. Setting $k_{20}=kt^{-\alpha}$ and changing the notation to substitute ϕ for C_1, the following fractal kinetic equation equivalent of Eq. (6) was derived:

$$\ddot{\phi} + (a + b + kt^{-\alpha})\dot{\phi} + akt^{-\alpha}\phi = 0, \quad (10)$$

where $a=k_{21}$ and $b=k_{12}$.

Using Eq. (10) in the analysis of data from four sets of instrumented dogs [14], the spectral dimension for the dog liver was estimated to be between 1.778 and 1.914, giving reasonable agreement with the available experimental data. However, this study was limited to the animal model and was tested for only one drug. Furthermore, a solution to Eq. (10) was determined only approximately, using perturbation theory, and was then fit numerically to the experimental data. In this paper, we further investigate the fractal two-compartment model, providing some exact analytical solutions as well as using numerical simulations for several sets

of experimentally determined parameters to generate a spectrum of fractal exponents that characterize the system. These exponents will be related to the shape of the long-time tail of the concentration profile, which allows its use as a diagnostic technique in, for example, the search for hepatic abnormalities.

II. ANALYTICAL SOLUTIONS

Fuite *et al.* [13] derived Eq. (10) as the basic modeling tool in the application of fractality to the pharmacokinetics of two-compartment models. Although Eq. (10) seems easily tractable at first glance, it in fact poses a serious mathematical challenge in the general case where the exponent α is a noninteger number. The approach applied by Fuite *et al.* in solving this equation was based on an approximate perturbative method of finding solutions that deviate only slightly from those obtained in the homogenously stirred case. While this method worked well in the case of mibefradil, there is no guarantee that it can be applied to a broad spectrum of drugs. In the present paper, we first examine the analytical solutions to Eq. (10) under special cases, before turning to numerical simulations performed for a wide range of drugs.

A. Case 1

We first consider the case where $\alpha=0$, which yields the classical two-compartmental model for homogeneously stirred compartments:

$$\ddot{\phi}+(a+b+k)\dot{\phi}+ak\phi=0. \tag{11}$$

The solution is expressed in general as a sum of exponentials:

$$\phi(t)=\exp\left[-\frac{t}{2}(a+b+k)\right]\left\{B_1\exp\left[\frac{t}{2}\sqrt{(a+b+k)^2-4ka}\right]+B_2\exp\left[-\frac{t}{2}\sqrt{(a+b+k)^2-4ka}\right]\right\}. \tag{12}$$

A set of elimination curves for a range of coefficients is illustrated in Fig. 3.

B. Case 2

In the special case when $\alpha=1$ in Eq. (10), which corresponds to highly heterogeneous kinetics, the basic equation can be written as

$$\ddot{\phi}+\left(a+b+\frac{k}{t}\right)\dot{\phi}+a\frac{k}{t}\phi=0. \tag{13}$$

This equation can be solved by postulating an ansatz in the form $\phi=uv$, dividing by v and imposing a convenient form for v to eliminate the coefficient of $\dot{u}$. It can be reduced to an equation for u that can be cast in the standard Whittaker form [16]. We then find solutions of the form

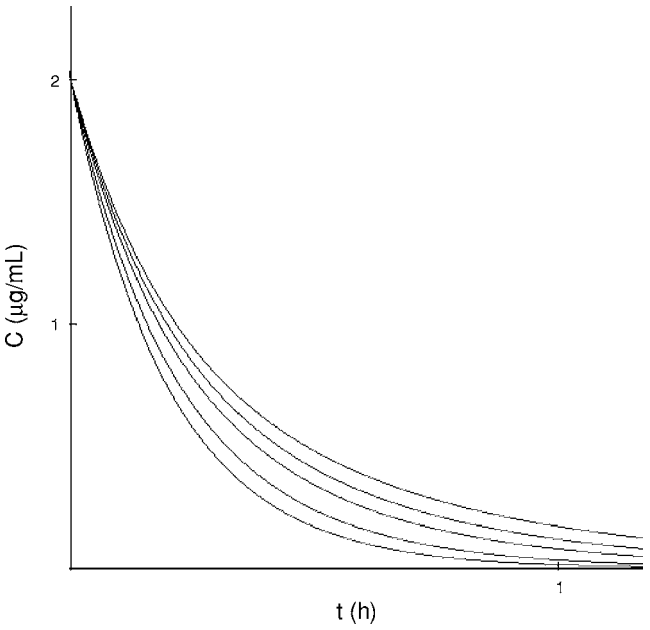

FIG. 3. A family of pharmacokinetic profiles, $C(t)$, showing elimination from a classical model following Eq. (3). The parameters were taken to be $a=2.0\ h^{-1}$, $b=5.0\ h^{-1}$, $B_1=1.0$, and $B_2=1.0$. The curves correspond to, from top to bottom, $k=0.05\ h^{-1}$, $k=0.5\ h^{-1}$, $k=1.0\ h^{-1}$, $k=2.0\ h^{-1}$, and $k=3.0\ h^{-1}$.

$$\phi(t)=c_1\Phi\left(\frac{ka}{a+b},k;-(a+b)t\right)+c_2t^{1-k}\Phi\left(1-\frac{kb}{a+b},2-k;-(a+b)t\right), \tag{14}$$

where c_1 and c_2 are integration constants and

$$\Phi(a,b;t)\equiv M(a,b;t)\equiv {}_1F_1(a,b;t) \tag{15}$$

is the Kummer function, or the Kummer confluent hypergeometric function. These functions can be cast into the Whittaker function form through the identity

$$M_{\sigma,\mu}(t)\equiv e^{-t/2}t^{\mu+1/2}{}_1F_1\left(\frac{1}{2}+\mu-\sigma,1+2\mu;t\right). \tag{16}$$

In the particular situation where $\alpha=1$ and $b=a$, we can simplify the solution to a form in terms of Bessel functions J_ν so that

$$\phi(t)=\left\{C_1\exp\left[\frac{i\pi}{4}(1-k)\right]\Gamma\left(\frac{1+k}{2}\right)e^{-at}\left(-\frac{at}{2}\right)^{(1-k)/2}\times J_{(-1+k)/2}(-iat)+C_2\exp\left[-\frac{i\pi}{4}(1-k)\right]\times\Gamma\left(\frac{3-k}{2}\right)e^{-at}\left(-\frac{2t}{a}\right)^{(1-k)/2}J_{(1-k)/2}(-iat)\right\}. \tag{17}$$

This solution exhibits a combination of exponential and power-law long-time asymptotics.

C. Case 3

The next special case considered that lends itself to an analytical solution to Eq. (10) involves taking $b=0$ (corresponding to fast clearance) so that the basic equation takes the form

$$\ddot{\phi} + (a + kt^{-\alpha})\dot{\phi} + akt^{-\alpha}\phi = 0. \tag{18}$$

Multiplying Eq. (18) on both sides by t^{α} and introducing a new dependent variable $F \equiv \dot{\phi} + a\phi$ reduces it to an integrable first-order equation

$$t^{\alpha}\dot{F} + kF = 0. \tag{19}$$

For $0 < \alpha < 1$, we can solve Eq. (19) to obtain

$$F = F_0 \exp\left(\frac{kt^{-\alpha+1}}{\alpha - 1}\right). \tag{20}$$

Hence

$$\phi(t) = C_1 e^{-at} + C_2 e^{-at} \int^t d\tilde{t} \exp\left[a\tilde{t} - \frac{k\tilde{t}^{1-\alpha}}{1-\alpha}\right]. \tag{21}$$

From Eq. (13), asymptotically, $\phi(t) \sim C_1 \exp[-at] + C_2$ as $t \to \infty$. For $\alpha = 1$, we find that

$$F = F_0 t^{-k} \tag{22}$$

and hence

$$\phi = e^{-at} \int^t F_0 \tilde{t}^{-k} e^{a\tilde{t}} d\tilde{t}. \tag{23}$$

For $0 \leqslant \alpha < 1 (\alpha \neq 1)$, we have

$$\phi(t) = \left[C_0 + C_1 \int^t d\tilde{t} \frac{\exp\left[-a\tilde{t} - \frac{k(\tilde{t})^{1-\alpha}}{1-\alpha}\right]}{(g(\tilde{t}))^2}\right] g(t), \tag{24}$$

where

$$g(t) = \frac{1}{a} - t - \left(\frac{1}{a}\right)\exp[-at] + t\ {}_1F_1\left[\frac{1}{1-\alpha}, \frac{1}{1-\alpha} + 1; \frac{-kt^{1-\alpha}}{1-\alpha}\right] + \sum_{p=1}^{\infty}\sum_{q=1}^{\infty} A_{p,q} t^{1+p+q(1-\alpha)},$$

$$A_{p,q} = \frac{-a[q(1-\alpha)+p]A_{p-1,q} - k[q(1-\alpha)+p+\alpha]A_{p,q-1} - kaA_{p-1,q-1}}{[q(1-\alpha)+p][q(1-\alpha)+p+1]}, \quad p \geqslant 1, \quad q \geqslant 1,$$

$$A_{p,0} = \frac{(-1)^p a^p}{(p+1)!},$$

$$A_{0,q} = \frac{(-1)^q k^q}{(1-\alpha)^{q+1}\left[\frac{1}{1-\alpha} + q\right] q!}. \tag{25}$$

Equation (24) represents a combination of exponential and stretched-exponential behavior superimposed with special functions.

D. Case 4

The situation where the rate of elimination exceeds the recycling rate (i.e., $a \gg b$, which is not as strong a condition as the one used in the previous case) leads to a number of tractable forms even for arbitrary α. The term in b is put on the right-hand side of Eq. (10) and the whole divided by $\dot{\phi} + a\phi$ (assumed $\neq 0$). Multiplying the numerator and denominator of the right-hand side by $1/a$ and assuming $1 \gg \dot{\phi}/a\phi$, we obtain a Bernoulli equation after one integration:

$$\dot{\phi} + a\phi = \exp\left[\frac{kt^{-\alpha+1}}{-\alpha+1} + d_0\right]\phi^{-b/a} \tag{26}$$

and we can integrate it to find

$$\phi = \left[\left(\frac{a+b}{a}\right)e^{-(a+b)t} \int^t e^{(a+b)\tilde{t}} \exp\left(\frac{k\tilde{t}^{-\alpha+1}}{-\alpha+1} + d_0\right) d\tilde{t}\right]^{a/(a+b)}. \tag{27}$$

When $a \gg b$ and $\alpha = 1$, we obtain another form of the Bernoulli equation: namely,

$$\dot{\phi} + a\phi = c_0 t^{-k}\phi^{-b/a}, \tag{28}$$

which can be interpreted to give

$$\phi = \left[\left(\frac{a+b}{a}\right)c_0 e^{-(a+b)t} \int^t \tilde{t}^{-k} e^{(a+b)\tilde{t}} d\tilde{t}\right]^{a/(a+b)}. \tag{29}$$

We note that a vast number of these solutions have exponential, stretched exponential, and/or power-law characteristics. In order to investigate these properties, we performed a numerical study of representative cases.

TABLE I. Values for the published kinetic coefficients for different drugs.

Reference	Drug	a (h^{-1})	b (h^{-1})	k (h^{-1})
[17]	EpsilonACA	0.035	0.023	0.022
[18]	C1-inhibitor protein	0.019	0.021	0.012
[19]	Ciprofloxacin	0.907	0.843	0.464
[20]	Ganciclovir	0.66	1.44	0.022
[21]	Ibuprofen	0.59	1.52	0.05
[19]	Ofloxacin	2.550	1.010	0.208
[22]	Transexamic acid	0.018	0.021	0.014

III. COMPUTER SIMULATIONS

We performed computer simulations of Eq. (10) for different values of the exponent α. All simulations were performed using Mathematica, version 3. Seven different sets of values for the kinetic rate coefficients a, b, and k were chosen from the pharmacological literature from papers reporting the applicability of two-compartment models to experimental data analysis. The trade names for the drugs as well as their associated parameters are listed in Table I. Both ε-aminocaproic (epsilonACA) and transexamic acid (TA) are used to reduce blood loss and the need for transfusion in cardiac surgery patients. The C1-inhibitor protein (C1-INH) is used to treat various conditions, including hereditary angioedema, acute myocardial infarction, and arthritis. Ciprofloxacin and ofloxacin are antimicrobials of the quinolone family, ganciclovir is used as a prophylaxis and antiviral agent, and ibuprofen is a nonsteroidal anti-inflammatory agent.

Initially, the second-order differential equation was solved numerically for each set of parameters for fractal exponents in the range $0 \leqslant \alpha \leqslant 0.1$, generating 11 curves for each of the 7 drugs. It was found that the long-time tail of the resulting concentration-versus-time curves was best described by a single exponential term. In order to characterize the effect of the fractal exponent α on the shape of the exponential tail,

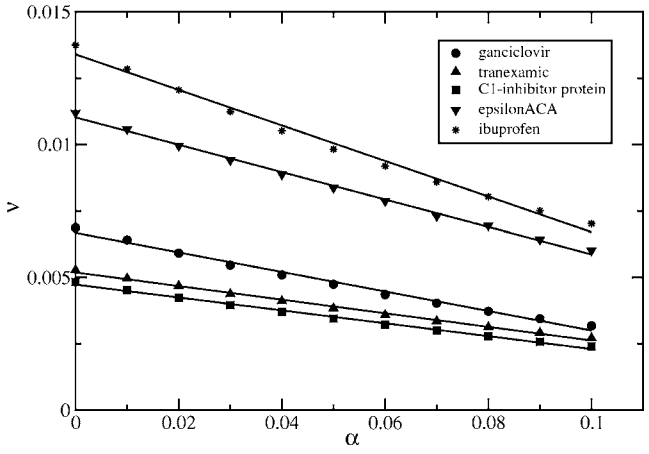

FIG. 4. The linear relationship between the exponential coefficient ν and α.

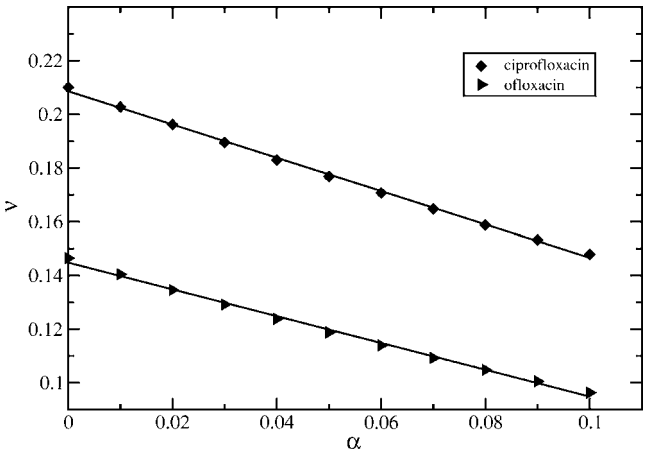

FIG. 5. The linear relationship between the exponential coefficient ν and α.

log-linear plots of the tails were generated and the resulting slope ν was calculated, where

$$C(t) \sim e^{-\nu t}. \tag{30}$$

Two composite plots (Figs. 4 and 5) of ν as a function of α show a linear relationship of the form

$$\nu = m(k)\alpha + n(k). \tag{31}$$

The values for the slope m and the y intercept n are listed in Table II. Based on a somewhat limited number of data sets, we have noticed that both m and n are linearly proportional to the elimination coefficient k. This argument requires further study.

The study was then repeated for higher values bracketing t^{-1}: namely, $0.95 \leqslant \alpha \leqslant 1.05$. It was found that in most cases, the elimination tail was now best described by a power law of the form

$$C(t) \sim t^{-\gamma}. \tag{32}$$

Figure 6 shows a plot of the power exponent γ as a function of α. In this case, the relationship between the two parameters is nonlinear, as might be expected since the behavior of the elimination tail undergoes a crossover as α is varied from close to zero to near unity.

Figure 7 compares the results for the drug ciprofloxacin in two different cases $\alpha = 0.05$ and $\alpha = 1.05$. The former pro-

TABLE II. Values for the slope and y intercept of ν versus α graphs.

Drug	Slope m	Intercept n	R^2
EpsilonACA	−0.0505 (0.0005)	0.01105 (0.0001)	0.9987
C1-inhibitor protein	−0.0236 (0.0004)	0.00468 (0.00007)	0.9976
Ciprofloxacin	−0.611 (0.002)	0.2080 (0.0007)	0.9995
Ganciclovir	−0.0356 (0.0007)	0.0066 (0.0001)	0.9959
Ibuprofen	−0.065 (0.001)	0.0132 (0.0002)	0.9964
Ofloxacin	−0.489 (0.003)	0.1441 (0.0009)	0.9986
Transexamic acid	−0.0251 (0.0003)	0.00515 (0.00007)	0.9978

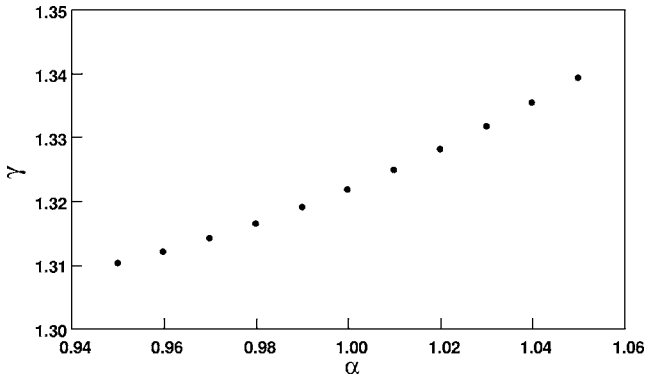

FIG. 6. The nonlinear relationship between the power-law exponent γ and α for ciprofloxacin.

duces a long-time exponential tail, while the latter produces a power-law tail. Therefore, two distinctly different types of behavior can be generated by a fractal, time-dependent elimination coefficient. In addition, it was found that in the case of ciprofloxacin, the transition from exponential to power-law behavior occurred at around $\alpha=0.5$, the value identified as the crossover point.

IV. DISCUSSION AND CONCLUSION

Fractality can occur in pharmacokinetic systems as a result of either the geometry of the eliminating organ or anomalous diffusion through constricted spaces (to be discussed in detail in a following paper). Previously [13], we showed that fractal elimination leads to power-law tails in the pharmacokinetic concentration profile. However, we have shown here that fractality can also be present in the case of exponential behavior. Our analytical treatment of the governing equation indicates that the actual form of the solution is mathematically complex, involving a host of special functions. Thus it is not surprising that elimination tails dominated by either an exponential or a power law can bear the hallmark of fractal kinetics.

We have shown above that there is a distinct relationship between the shape of the elimination tail (characterized by either ν or γ) and the fractal exponent α; in the case of very small α, the relationship is nicely linear. Therefore, we should be able to extract knowledge about the underlying fractal kinetics of a system by analyzing the long-time tail of

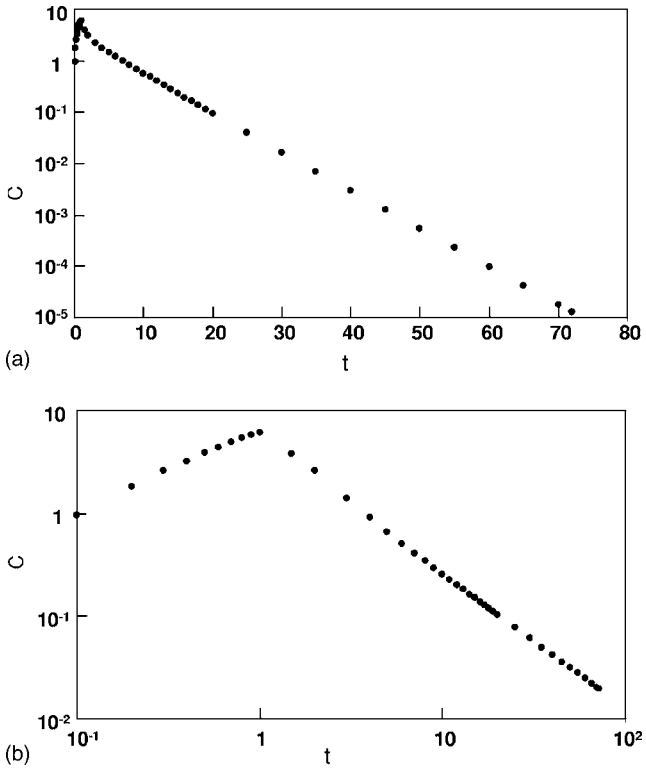

FIG. 7. Pharmacokinetic concentration profiles for ciprofloxacin for (a) $\alpha=0.05$, showing an exponential tail ($\nu=0.1739\pm0.0004$), and (b) $\alpha=1.05$, showing a power-law tail ($\gamma=1.339\pm0.006$).

the pharmacokinetic profile. While small deviations from classical kinetics still retain exponential behavior, there is a value of α where a transition to a power law occurs. Because a higher value of α indicates a greater deviation from classical kinetics ($\alpha=0$), this appearance and growth of power-law behavior should be related to the complexity of the underlying system. Consequently, a potentially important application of this work is in quantifying the correlation between the body's pharmacokinetic response and its state of health (such as liver function).

ACKNOWLEDGMENTS

This research was supported by grants from NSERC and MITACS (project title "Mathematical Modeling and Pharmaceutical Development"). J.M.D. and P.C. received support for their positions at the University of Alberta from the Theoretical Physics Institute.

[1] M. Gibaldi and D. Perrier, *Pharmacokinetics*, 2nd ed. (Marcel Dekker, New York, 1982).
[2] J. A. Jacquez, *Compartmental Analysis in Biology and Medicine*, 3rd ed. (BioMedware, Ann Arbor, 1996).
[3] P. Grassberger and I. J. Procaccia, Chem. Phys. **77**, 6281 (1982).
[4] L. W. Anacker, R. J. Kopelman, and J. S. Newhouse, J. Stat. Phys. **36**, 591 (1984).
[5] L. W. Anacker and R. J. Kopelman, Chem. Phys. **81**, 6402 (1984).
[6] R. J. Kopelman, J. Stat. Phys. **42**, 185 (1986).
[7] R. J. Kopelman, Science **241**, 1620 (1988).
[8] P. Argyrakis and R. J. Kopelman, J. Phys. Chem. **93**, 225 (1989).
[9] M. J. Weiss, J. Phys. Chem. **27**, 383 (1999).
[10] P. Macheras, Pharm. Res. **13**, 663 (1996).
[11] V. Karalis, L. Claret, A. Iliadis, and P. Macheras, Pharm. Res. **18**, 1056 (2001).

[12] V. Karalis and P. Macheras, Pharm. Res. **19**, 697 (2002).
[13] J. Fuite, R. Marsh, and J. Tuszynski, Phys. Rev. E **66**, 021904 (2002).
[14] A. Skerjanec, S. Tawfik, and Y. K. Tam, J. Pharm. Sci. **85**, 189 (1995).
[15] C. J. Javanaud, J. Acoust. Soc. Am. **86**, 493 (1989).
[16] I. S. Gradshteyn and I. M. Ryzhik, *Table of Integrals, Series, and Products* (Academic Press, San Diego, 2000).
[17] D. G. Ririe, R. L. James, M. J. O'Brien, Y. A. Lin, J. Bennett, D. Barclay, M. H. Hines, and J. F. Butterworth, Anesth. Analg. (Baltimore) **94**, 44 (2002).
[18] J. H. Diris, W. Th. Hermens, P. W. Hemker, W. K. Lagrand, C. E. Hack, and M. P. van Dieijen-Visser, Clin. Pharmacol. Ther. **72**, 498 (2002).
[19] F. Khorasheh, S. Sattari, A. Gerayeli, and A. M. Ahmadi, J. Pharm. Pharm. Sci. **2**, 92 (1999).
[20] D. Czock, C. Scholle, F. M. Rasche, D. Schaarschmidt, and F. Keller, Clin. Pharmacol. Ther. **72**, 142 (2002).
[21] B. van Overmeire, D. Touw, P. J. C. Schepens, G. L. Kearns, and J. N. van den Anker, Clin. Pharmacol. Ther. **70**, 336 (2001).
[22] N. P. Dowd, J. M. Karski, D. C. Cheng, J. A. Carroll, Y. Lin, R. L. James, and J. Butterworth, Anesthesiology **97**, 390 (2002).